Macromol. Symp. ***157,*** *225–237 (2000)*

Synthesis and Solution Properties of Star-Shaped Poly(*tert*-butyl acrylate)

Daniela Held[a] ***and Axel H. E. Müller***[a,b*]

[a] Institut für Physikalische Chemie, Universität Mainz, Welderweg 15, D-55099 Mainz, Germany

[b] Makromolekulare Chemie II and Bayreuther Institut für Makromolekülforschung, Universität Bayreuth D-95440 Bayreuth, Germany. E-mail: axel.mueller@uni-bayreuth.de

Abstract:

A series of star polymers consisting of poly(*tert*-butyl acrylate) arms and an ethyleneglycol dimethacrylate (EGDMA) microgel core were synthesized using anionic polymerization. The effect of various parameters (precursor length, ratio [EGDMA]/[Initiator], reaction time, and overall concentrations) on the average number of arms was investigated. Molecular weights were determined using GPC coupled with an online viscometer and MALLS. The exponents for the relation between intrinsic viscosity or radius of gyration and molecular weight, respectively, are extremely low, indicating that the dimensions of the star polymers only slightly increase with the number of arms. After a certain number of arms is reached the intrinsic viscosity even decreases with molecular weight. Computer simulations for star polymers were carried out where the radius of gyration was calculated as a function of the number of arms. The results are in good agreement with the experimental data.

Introduction

Branched structures have been the subject of continuing interest in polymer chemistry. Besides randomly branched, comb-shaped and hyperbranched polymers, star-shaped polymers have been investigated for several years[1]. Star polymers consist of linear chains connected to one single junction point referred to as core. There are different ways to obtain a star polymer using controlled polymerization. In order to obtain a defined number of arms per molecule, multifunctional initiators or termination reagents have been used, mostly to form polystyrene or polydiene stars[2]. However, this method was not really successful for polar monomers like (meth)acrylates, because of the reduced reactivity towards the multifunctional termination reagents at the low temperatures needed for controlled polymerization[3]. Another possibility is the use of a difunctional monomer like divinylbenzene, either to form a plurifunctional initiator by reaction with a monofunctional one (core first)[4] or by coupling with active chain ends (arm first)[5]. Stars produced in such a way have a broad distribution of the number of arms. An advantage of the arm-first method is that it is possible to isolate and

CCC 1022-1360/00/$ 17.50+.50/0

characterize the polymer chains which become the arms of the resulting star. The average number of arms, f, is therefore easily determined when the molecular weight of the star polymer is known.

During the last decade PMMA star polymers were synthesized using GTP or anionic polymerization[6,7]. The bifunctional monomer used here was ethyleneglycol dimethacrylate (EGDMA). The polymers were often characterized by GPC coupled with viscosity or multi-angle laser light scattering (MALLS) detectors. Poly(*tert*-butyl acrylate) (P*t*BuA) star polymers were also prepared but here a different method was used[8]. Short polystyrene chains were coupled with divinylbenzene (arm-first) and the resulting active centers in the core were used to initiate the living anionic polymerization of *t*BuA. Therefore star polymers with two different kinds of arms and a very non-polar core were achieved. The effect of various parameters, i. e., precursor length, ratio [EGDMA]/[Initiator] ($[E]_0/[I]_0$) and overall concentration, on star formation and on the average number of arms, f, is still under discussion in literature. Mays[9], Burchard[10] and Higashimura[11] and their coworkers found that the number of arms increases with the ratio $[E]_0/[I]_0$. The two latter groups also claimed a decrease of f with increasing arm molecular weight. For star polymers produced by GTP Haddleton and Crossman[12] found that the number of arms is not related to the arm length. For the stars made by anionic polymerization they emphasize the important role of the overall concentrations[13]. Higher overall concentrations lead to a higher average number of arms.

Compared to their linear analogues with the same molecular weight branched polymers have smaller dimensions leading to a reduced viscosity. This effect becomes more pronounced with increasing number of branches. Nevertheless, the exponent of the relation between intrinsic viscosity and molecular weight, $[\eta] = K \cdot M^{\alpha}$, is the same for a linear polymer and a star with a constant number of arms[14]. This means that in a Mark-Houwink plot a star polymer which grows by adding monomer to the arms, results in a parallel line to the linear one, but shifted to lower viscosity. The Mark-Houwink exponent, α, depends on the structure of the polymer in solution. Its value can be in the range from 0 (solid sphere) to 2 (rigid rod). For the relation between the radius of gyration and molecular weight of star polymers in good solvent Daoud and Cotton[15] calculated a dependence of $R_g \propto N^{0.6}\ f^{0.2}$ (N = number of segments per arm). For N = const. this results in $R_g \propto M^{0.2}$. Stars made by the arm-first approach with a bifunctional monomer have an interesting feature, because they do not have a constant number of arms. Here the molecular weight increases by adding arms and therefore the structure changes within the sample. This should result in a smaller exponent in a plot analogous to a Mark-Houwink plot[16].

In this work star polymers with P*t*BuA arms were prepared via the arm-first strategy using EGDMA as a linking agent. P*t*BuA stars are convenient starting materials for the synthesis of poly(acrylic acid) stars. Furthermore, the molecular parameters in solution, the exponent of the intrinsic viscosity vs. molecular weight, α, and the exponent for the relation between the radius of gyration and molecular weight, α_s, were determined using a viscometer and MALLS coupled with GPC.

Experimental Part

Reagents: Diphenylethylene (DPE) was purified by adding n-butyllithium until the solution turned slightly red followed by distillation. Diphenylhexyllithium (DPHLi) was prepared by adding n-butyllithium (1.6 M solution in hexane) to an excess of DPE in hexane. The solution was stirred at room temperature until the DPHLi precipitated. The red solid was isolated and washed with hexane several times. At last the initiator was dried on the vacuum line and stored under nitrogen. LiCl (Merck) was dried in high vacuum at 300 °C for two days. *tert*-Butyl acrylate (*t*BuA, BASF AG) was fractionated from CaH_2 over a 1 m column filled with Sulzer packing at 45 mbar, stirred over CaH_2, degassed and distilled in high vacuum just before use. Ethyleneglycol dimethacrylate (Röhm GmbH) was fractionated over a 10 cm Vigreux column, stirred over CaH_2, distilled in high vacuum and filtrated over a short column filled with dry neutral alumina. Decane (internal standard for GC, Aldrich) was stirred over sodium/potassium alloy, degassed and distilled on the vacuum line. THF (BASF AG) was fractionated over a 1.5 m column, stirred twice over sodium/potassium alloy, degassed and distilled on the vacuum line.

Polymerization: All experiments were carried out in a stirred tank reactor under nitrogen atmosphere. The initiator ($[I]_0 = 1 \cdot 10^{-3}$ mol/l) and a fivefold molar excess of LiCl dissolved in THF were introduced and cooled to –78°C. Then *t*BuA was added. After 5 min reaction time a sample (precursor) was taken and EGDMA was introduced. After 10 min. a first sample was taken. The polymerization was quenched after 90 min with acidic methanol. Conversion of EGDMA (x_E) was measured by gas chromatography. The polymers were isolated by precipitation into methanol/water (50/50). It was dried under vacuum at room temperature for at least 2 days.

Characterization: GPC measurements were performed at room temperature using 5 μ PSS SDV gel columns (column set: 10^3, 10^5, 10^6 Å) with THF as eluent at a flow rate of 0.5 ml/min. Detectors: Applied Biosystems 1000S UV diode-array detector; Wyatt Technology DAWN-DSP F multiangle laser light scattering instrument equipped with an He-Ne laser (λ = 633 nm); Viscotek viscosity detector H 502B; Shodex refractive index detector (tungsten lamp) or NFT ScanRef scanning refractometer (λ = 633 nm) for online-determination of the refractive index increment. The average molecular weights of the star polymers were determined using GPC-Viscosity coupling.

Simulations: Monte-Carlo simulations were performed on a diamond lattice using a program developed by W. Radke[17].

Results and Discussion

Synthesis

A series of star polymers with P*t*BuA arms were synthesized using EGDMA as a linking agent. The precursor length was one of the investigated parameters. Therefore two different precursors with $M_w \approx 20{,}000$ and $M_w \approx 90{,}000$ were synthesized. The reaction time chosen for all precursors was 5 min. Efficient stirring is necessary because the reaction is extremely fast. The reaction time for the linking agent EGDMA was 90 minutes, after 10 minutes a sample was taken. All samples were characterized using GPC coupled with a viscometer and a MALLS detector. The refractive index increment dn/dc, was determined using a scanning interferometer. The samples were not fractionated which means that unreacted precursor is still present. However the average molecular weights of the star polymers could be determined by subtracting the residual precursor from the GPC eluograms. The number- and weight-average numbers of arms were calculated as

$$f_n = M_{n,star}\cdot(1-w_{core})/M_{n,arm} \quad \text{and} \quad f_w = M_{w,star}\cdot(1-w_{core})/M_{n,arm}.$$

The weight fraction of the core was calculated as $w_{core} = m_E\cdot x_E/[m_E x_E + m_{tBuA}\cdot(1-w_{prec})]$ where w_{prec} is the fraction of residual precursor in the eluogram.

First, the ratio $[E]_0/[I]_0$ was varied for two different arm molecular weights while the arm length, the reaction time and the initiator concentration were kept constant. For the low molecular weight precursors star polymers with only 3 - 6 % residual arms are formed after 90 min, as shown in Figure 1.

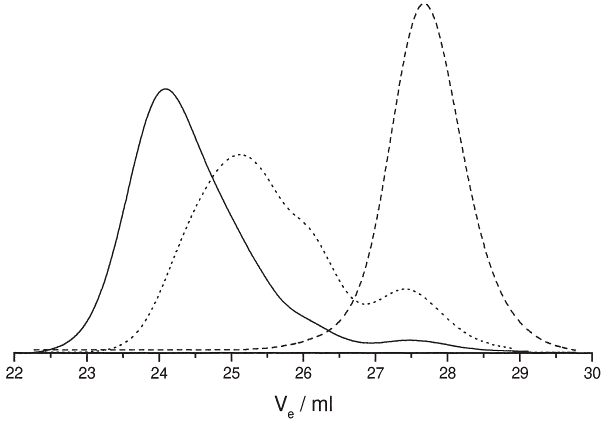

Figure 1: GPC eluograms of a low molecular weight precursor (M_w = 20,000) and the resulting star polymers after 10 and 90 min; $[E]_0/[I]_0 = 15$

For the high molecular weight precursors the content of residual arms decreases from 32% to 18% with increasing ratio $[E]_0/[I]_0$. Figure 2 shows the GPC eluograms of a sample with high precursor molecular weight and $[E]_0/[I]_0 = 15$ for different reaction times. The star formation is significantly slower; after 10 minutes most of the polymer consists only of precursor, dimer and trimer.

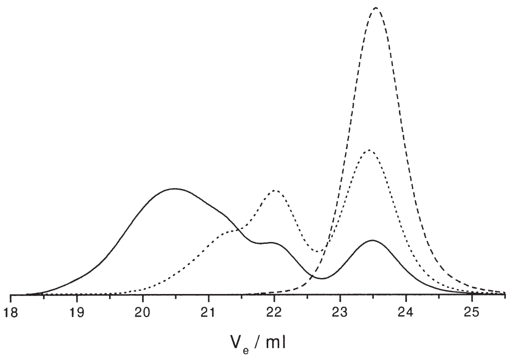

Figure 2: GPC eluograms of a high molecular weight precursor (---) and the resulting star polymers after 10 (·····) and 90 (—) min; $[E]_0/[I]_0 = 15$

Table 1 shows the dependence of the average number of arms on various parameters. f_w decreases with the length of the precursor and increases with reaction time and ratio $[E]_0/[I]_0$.

Table 1: Experimental conditions and results for star polymers with short and long precursor for different ratios $[EGDMA]_0/[I]_0$ and different reaction times. $[I]_0 = 1\cdot10^{-3}$ mol/l

$M_{n,Pre}\cdot10^{-4}$ (M_w/M_n)	$[E]_0/[I]_0$	t, min	$M_n\cdot10^{-4}$	$M_w\cdot10^{-4}$	$1-w_{core}$	f_n	f_w	x_E	w_{Prec}
1.80 (1.08)	5	10	4.08	4.63	0.88	1.99	2.26	0.77	0.42
		90	6.43	8.18	0.90	3.22	4.10	1.00	0.60
1.71 (1.09)	10	10	6.29	7.93	0.84	3.09	3.89	0.81	0.10
		90	8.65	11.5	0.83	4.20	5.59	1.00	0.04
1.70 (1.09)	15	10	5.91	7.30	0.81	2.81	3.47	0.64	0.11
		90	9.61	12.9	0.78	4.39	5.88	0.94	0.03
9.64 (1.06)	5	10	18.6	20.7	0.94	1.82	2.03	0.69	> 0.50
		90	27.1	37.8	0.97	2.74	3.82	0.90	0.32
10.5 (1.03)	10	10	21.3	27.5	0.95	1.93	2.49	0.65	0.48
		90	31.5	47.2	0.96	2.87	4.30	0.89	0.23
10.5 (1.04)	15	10	22.0	26.0	0.93	1.95	2.31	0.60	0.50
		90	36.2	54.8	0.94	3.24	4.91	0.83	0.18

For the high molecular weight precursors the conversion of EGDMA was not complete after 90 minutes reaction time. Therefore experiments were performed where the reaction time was increased up to 24 hours. This leads to nearly full conversion of the crosslinker. The average number of arms still increased with time while the content of residual precursor decreased (Table 2). Furthermore, an experiment was carried out, where the overall concentrations of the reagents was doubled ($[I]_0 = 2\cdot10^{-3}$ mol/l). This had a strong effect on the average number of arms. f_w is nearly twice as high as compared to the experiment with the low concentrations.

Table 2: Experimental conditions and results for star polymers with long precursors and ratio $[E]_0/[I]_0 = 15$

$M_{n,Pre}\cdot10^{-4}$ (M_w/M_n)	$[I]_0\cdot10^3$, mol/l	t, min	$M_n\cdot10^{-4}$	$M_w\cdot10^{-4}$	$1-w_{core}$	f_n	x_E	w_{Prec}
8.60 (1.04)	1	10	15.6	17.6	0.93	1.69	0.55	0.57
		90	27.8	39.0	0.94	3.05	0.86	0.17
		1275	44.9	63.6	0.94	4.91	0.97	0.11
7.94 (1.04)	2	10	20.4	26.9	0.95	2.45	0.62	0.28
		90	37.4	56.7	0.94	4.44	0.90	0.13
		1440	74.0	105	0.94	8.76	1.00	0.10

The eluograms for the experiments with the higher initiator concentration are shown in Figure 3. A shoulder is observed at extremely high molecular weight. This is assigned to a coupling reaction of two star molecules occurring between the anions of one core with unreacted vinyl groups of another one.

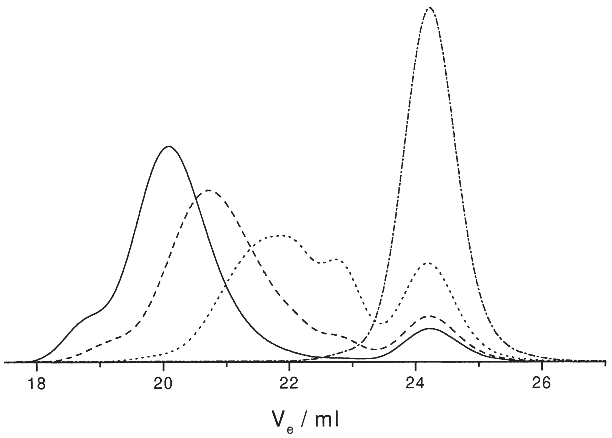

Figure 3: GPC eluograms; precursor (-·-·), 10 (·····), 90 (---) and 1440 (—) min reaction time with EGDMA; $M_{w,Pre} = 72000$; $[E]_0/[I]_0 = 15$; $[I]_0 = 2\cdot10^{-3}$ mol/l

Characterization

Intrinsic viscosity. Two different methods were used to obtain a Mark-Houwink plot and to calculate the exponent, α. First, it was determined from GPC coupled with a viscometer using a sample with a broad molecular weight distribution and, alternatively, from M_w and [η] of various star polymers of the same run taken at different reaction times. In both cases extremely small values ($0 < \alpha < 0,1$) are obtained, even when the average number of arms is low. The results are summarized with the results from GPC-MALLS in Table 3. The plots (Figure 4 and Figure 5) (both 90 min reaction time) also show the signal of the specific viscosity and the contraction factor $g' = ([\eta]_{branched}/[\eta]_{linear})_M$. Independently of the arm molecular weight the intrinsic viscosity decreases for star polymers down to 20% compared to a linear polymer with the same molecular weight. Figure 5 shows data for a star obtained from a precursor with high molecular weight. The signals for the precursor, the dimer, and trimer are still present after 90 min reaction time for crosslinking.

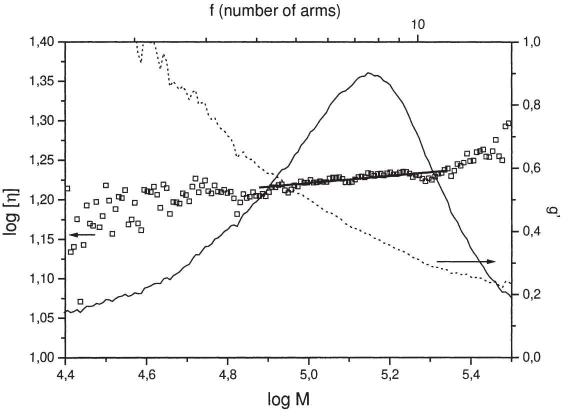

Figure 4: Mark-Houwink plot for a star polymer with short precursors ($M_w = 20,000$) and $[E]_0/[I]_0 = 15$; intrinsic viscosity (□), specific viscosity (—) and contraction factor, g' (·····), in dependence of molecular weight (or number of arms) in THF at 30 °C; $\alpha = 0.045$.

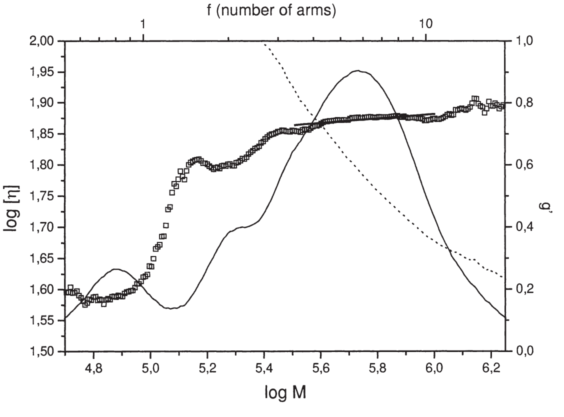

Figure 5: Mark-Houwink plot for a star polymer with long precursors ($M_w = 90,000$) and ratio $[E]_0/[I]_0 = 15$; $\alpha = 0.036$.

For star polymers with high molecular weight (high number of arms) we even observe negative exponents (Figure 6), which means that stars with higher molecular weight have a lower intrinsic viscosity.

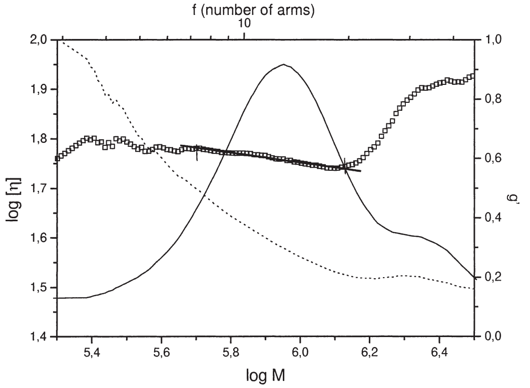

Figure 6: Mark-Houwink plot for a star polymer with long precursors ($M_w = 90,000$) and $[E]_0/[I]_0 = 15$; $[I]_0 = 2$ x10-3 mol/l; $\alpha = -0.10$.

It seems that for high molecular weight stars a negative exponent is obtained and for stars with less arms (and low molecular weight) a small, positive exponent. Therefore there should be a maximum in the plot of intrinsic viscosity vs. molecular weight. To detect the maximum of the intrinsic viscosity a mixture of samples taken at different reaction times was used to achieve a sample with a broad arm number distribution. In Figure 7 the maximum of the intrinsic viscosity, which is also implied in Figure 5, can be clearly seen.

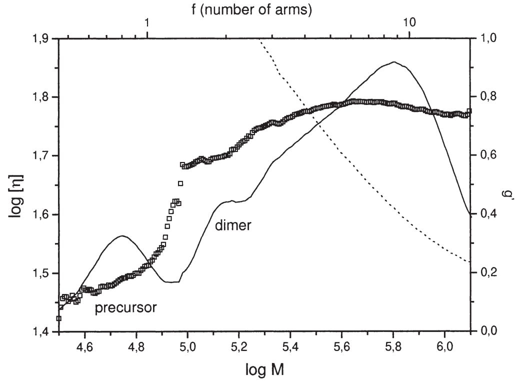

Figure 7: Mark-Houwink plot for a mixture of star polymer samples after 10, 90 and 1440 minutes reaction time; $[E]_0/[I]_0 = 15$; $[I]_0 = 2 \times 10^{-3}$ mol/l.

The maximum of the intrinsic viscosity can also be seen in the plot of log [η] vs. log M_w for samples of the same precursor taken at different reaction times (Figure 8).

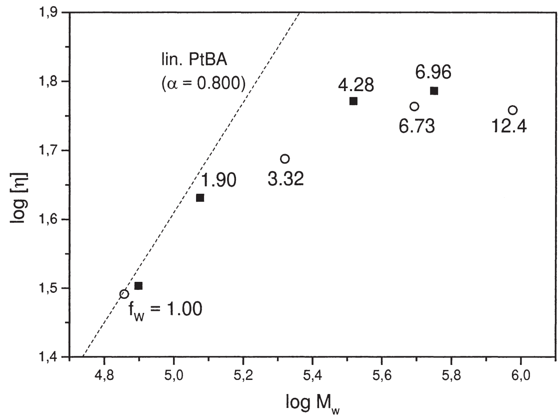

Figure 8: Mark-Houwink plot of high molecular weight precursor and samples after 10, 90 and 1440 minutes; $[E]_0/[I]_0 = 15$; (■): $[I]_0 = 1\cdot10^{-3}$ mol/l, (○): $[I]_0 = 2\cdot10^{-3}$ mol/l; (----): slope for linear P*t*BuA[18]

A maximum of the intrinsic viscosity has also been observed for dendrimers[19-21]. Here, the maximum occurs in the third generation, G = 3. At higher generations the intrinsic viscosity decreases with molecular weight. This is explained with a change in structure. After the addition of certain generations the dendrimer behaves like a sphere and can be described by Einstein's law: $[\eta]= 2.5V_h/M$. While adding the new generation the increase of the hydrodynamic volume, $V_h \propto G^3$, is smaller than the increase of molecular weight, $\log M \propto G$ and therefore $[\eta]$ decreases. This is due to the fact that the density in the center of the dendrimer is much smaller than in the outer sphere. For the star polymers the density is also changing but here the density in the inner region is much higher than in the outer. After a certain number of arms are added the increase of V_h is only very small but molecular weight still increases linearly. Another difference between these star polymers and dendrimers is that the star polymers are not self-similar. The structure is not constant while arms are added, and therefore the obtained exponent α in the Mark-Houwink plot is not constant either. It cannot be used to draw conclusions on the shape of the polymer in solution.

Light scattering. The characterization of the star polymers with short arms (low molecular weight precursor) by GPC-MALLS was not possible. The scattering signal in THF is too small because of the small refractive index increment of P*t*BuA (dn/dc = 0.059 ml/g) and the low molecular weight. The stars with the longer arms were analyzed using additionally an online scanning interferometer to determine dn/dc. In analogy to the viscosity measurements, the relation between the radius of gyration and the molecular weight was investigated. The molecular weights determined by GPC-MALLS are summarized in Table 3 together with the exponents α and α_S, the exponent of the relation R_g vs. molecular weight. In Figure 9 the concentration signal and the radius of gyration vs. the molecular weight can be seen. There are reasonable results only for M > 300,000. The radius of gyration increases only slightly with the number of arms.

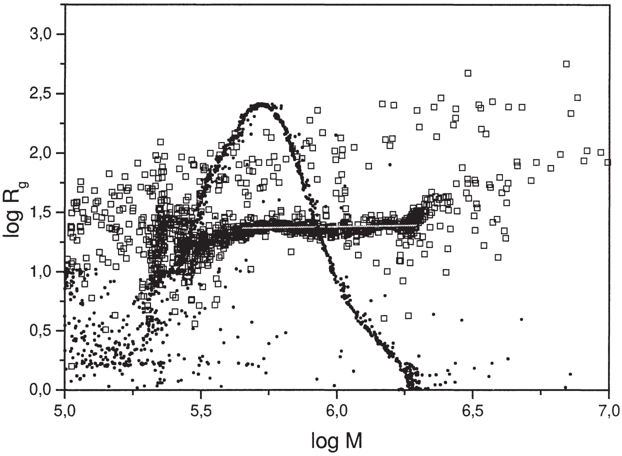

Figure 9: Radius of gyration (□) for a star polymer with long precursor; $[E]_0/[I]_0 = 15$; $[I]_0 = 1 \cdot 10^{-3}$ mol/l; (•): concentration signal; $\alpha_s = 0.038$.

The analysis is quite difficult due to the fact that there is no scattering signal for the residual precursor. This also poses problems in the determination of the molecular weight averages. M_n and M_w obtained from GPC-MALLS are always higher than those derived from GPC-viscosity using a universal calibration curve and determined for the whole sample including the residual precursor (Table 3). This results in a considerable error in M_n due to undetectable residual precursor. Nevertheless, the values for M_w are within 15 % error compared to GPC-viscosity indicating that GPC separation is working for these polymers, even when the previous results showed that the dimensions of the stars only slightly increase with molecular weight (i. e., number of arms). For reliable universal calibration the separation of the polymers is required because the method is only relative and a calibration curve and monodisperse slices are needed. GPC-MALLS is an absolute method and the obtained M_w values should be correct even if the GPC columns are not able to properly separate molecules with different arm numbers. Nevertheless the separation is needed for the correct determination of the exponent α_s. If the slices are polydisperse the weight-average of the molecular weight and the z-average of the radius of gyration are compared in every slice and this can cause an error in the evaluation[22].

The obtained exponents, α_s, are extremely low and smaller than for hard spheres with constant density ($\alpha_s = 0.33$). However, they are in the range calculated by Daoud and Cotton ($\alpha_s = 0.2$).

Table 3: Molecular weights and scaling exponents obtained from GPC-MALLS and GPC-viscosity coupling

$M_{w,Pre}\cdot10^{-4}$	$[E]_0/[I]_0$	$[I]_0\cdot10^3$, mol/l	t, min	$M_w\cdot10^{-5}$ (GPC-MALLS)	deviation to M_w (GPC-visco)^a %	α_S	α
10.2	5	1	90	3.04	9	-	0.129
10.9	10	1	90	4.19	13	0.140	0.032
10.9	15	1	90	5.03	12	0.038	0.036
8.90	15	2	90	5.27	7	0.198	-0.062
8.28	15	2	1440	10.6	12	0.233 0.787^b	-0.099

[a] for the sample including the residual precursor, therefore M_w and especially M_n are lower than the average molecular weights given in Table 1 and Table 2
[b] high molecular weight peak

Figure 10 shows a plot of radius of gyration vs. molecular weight with two different slopes. For the "normal" star polymers a small exponent is observed ($\alpha_s = 0.233$). However, for $M > 10^6$ a much higher value is found ($\alpha_s = 0.787$). This may be due to a structural change. These polymers probably are coupled stars formed by core-core coupling which may be more ellipsoid than normal stars.

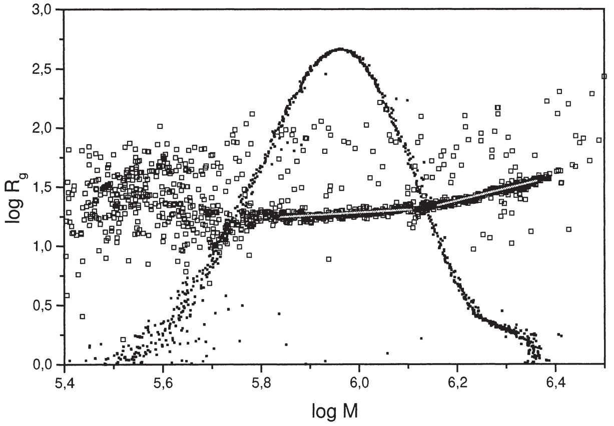

Figure 10: Determination of α_S for a sample with a high molecular weight precursor ($M_w = 72{,}000$) and star-star coupling; $[E]_0/[I]_0 = 15$; $[I]_0 = 2\cdot10^{-3}$ mol/l

Computer Simulations

Computer simulations were performed in order to confirm the obtained low values for α_s. The radius of gyration was calculated for star polymers in a good solvent with constant number of segments per arm, N_{arm}, and different number of arms, f. From the plot of radius of gyration vs. total number of segments of the star polymer, N, (Figure 11) α_s can be calculated. The obtained values are very low and decrease with increasing number of segments per arm.

These results are in good agreement with the experimental data and indicates even smaller scaling factors than predicted by Daoud and Cotton.

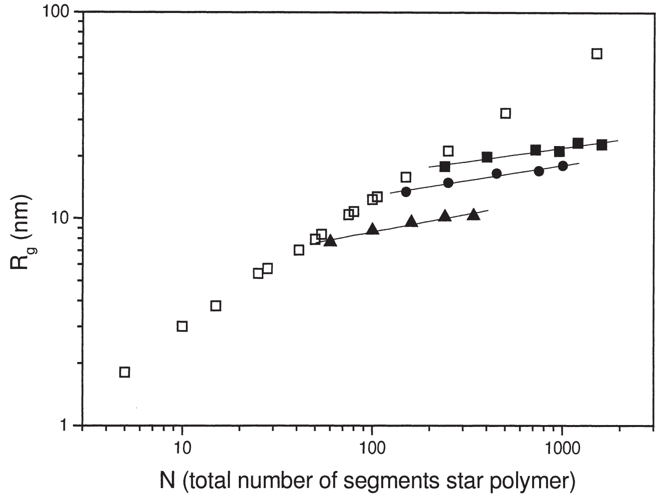

Figure 11: Results of computer simulation of star polymers with constant arm length, N_{arm}. (□) linear polymer; $\alpha_s = 0.616$; (▲) $N_{arm} = 20$; f = 3-17; $\alpha_s = 0.172$; (●) $N_{arm} = 50$; f = 3-20; $\alpha_s = 0.147$; (■) $N_{arm} = 80$; f = 3-20; $\alpha_s = 0.133$

Conclusions

For P*t*BuA star polymers with EGDMA core the precursor length, the ratio $[E]_0/[I]_0$ and the reaction time for the bifunctional monomer influence the average number of arms. This is in agreement with results of Mays, Burchard and Higashimura and their groups. The most important factor affecting the average number of arms is the overall concentration. Doubling of the concentrations resulted in star polymers with nearly doubled average number of arms. The amount of residual precursor decreases with decreasing precursor length, increasing time and increasing ratio $[EGDMA]_0/[I]_0$. All star polymers have a quite narrow arm number distribution. The viscosity behavior of the stars is similar to that of dendrimers. The intrinsic viscosity passes a maximum, it decreases after a certain number of arms is reached. In contrast to dendrimers the radius of gyration increases only slightly with molecular weight. This results in a low scaling exponent as predicted by Daoud and Cotton. The experimental data are in good agreement with simulations performed for star polymers in a good solvent.

Acknowledgement: This work was supported by the *Deutsche Forschungsgemeinschaft* within the *Schwerpunktsprogramm "Polyelektrolyte"*. The authors thank Dr. Wolfgang Radke (DKI, Darmstadt) for helpful discussions.

References

1) S. Bywater, *Adv. Polym. Sci.* **30**, 89 (1979)
2) M. Morton, T. E. Helminiak, S. D. Gadkary, F. J. Bueche, *J Polym. Sci.* **57**, 471 (1962)
3) N. Hadjichristidis, *J. Polym. Sci., Part A.* **37**, 857 (1999)
4) H. Eschwey, M. L. Hallensleben, W. Burchard, *Makromol. Chem.* **173**, 235 (1973)
5) J.-G. Zilliox, P. Rempp, J. Parrod, *J Polym. Sci.: Part C* **22**, 145-156 (1968)
6) PCT Patent WO 86/00626 (1986), E. I. du Pont de Nemours & Co., inv. J. H. Spinelli
7) J. A. Simms, *Rubber Chemistry And Technology* **64**, 139 (1991)
8) C. Tsitsilianis, P. Lutz, S. Graff, J. P. Lamps, P. Rempp, *Macromolecules* **24**, 5897 (1991)
9) V. Efstratiadis, G. Tselikas, N. Hadjichristidis, J. Li, Y. Wan, J. W. Mays, *Polym. Int.* **33**, 171 (1994)
10) P. Lang, W. Burchard, M. S. Wolfe, H. J. Spinelli, L. Page, *Macromolecules* **24**, 1306 (1991)
11) S. Kanoka, M. Sawamoto, T. Higashimura, *Macromolecules* **24**, 2309 (1991)
12) D. M. Haddleton, M. C. Crossman, *Macromol. Chem. Phys.* **198**, 871 (1997)
13) M. C. Crossman, D. M. Haddleton, *Macromol. Symp.* **132**, 187 (1998)
14) J. Roovers, L.-L. Zhou, P. M. Toporowski, M. van der Zwan, H. Iatrou, N. Hadjichristidis, *Macromolecules* **26**, 4324 (1993)
15) M. Daoud, J. P. Cotton, *Journal de Physique* **43**, 531 (1982)
16) W. Burchard, *Adv. Polym. Sci.* **143**, 113 (1999)
17) W. Radke, Dissertation, Universität Mainz Mainz 1996
18) L. Mrkvicková, J. Danhelka, *J. Appl. Polym. Sci.* **41**, 1929 (1990)
19) O. Lambert, P. Dumas, G. Hurtrez, G. Riess, *Macromol. Rapid Commun.* **18**, 343-351 (1997)
20) C. Cai, Z. Y. Chen, *Macromolecules* **31**, 6393 (1998)
21) F. Bohlmann, J. Jacob, *Chem. Ber.* **107**, 2578 (1974)
22) M. Wintermantel, M. Gerle, K. Fischer, M. Schmidt, I. Wataoka, K. Urakawa, Y. Tsukahara, *Macromolecules* **29**, 978 (1996)